JPP Journal of Pharmacy and Pharmacology

JPP 2007, 59: 637–643

Received November 7, 2006
Accepted January 29, 2007
DOI 10.1211/jpp.59.5.0003
ISSN 0022-3573

Analysis of eupatilin–human serum albumin interactions by means of spectroscopic and computational modelling

Jianghong Tang, Ning Lian, Chenglu Bi and Weihua Li

Abstract

The interaction of eupatilin (5,7-dihydroxy-3′,4′,6-trimethoxyflavone) with human serum albumin (HSA) was studied at simulative physiological pH, with a HSA concentration of 3.0×10^{-6} mol L^{-1} and eupatilin concentrations over the range of 6.0×10^{-6} to 1.9×10^{-5} mol L^{-1}. Fluorescence spectroscopy in combination with UV absorption spectroscopy and Fourier transform infrared (FTIR) spectroscopy were used to study the binding properties (including binding mechanism, the binding constants, the number of binding sites and the binding mode) of the interaction of eupatilin with HSA and the effect of this drug on HSA conformation changes. According to the Scatchard equation there was only one class of binding site that could bind to HAS; the binding constants were 1.53×10^5, 1.20×10^5, 1.05×10^5, 0.87×10^5 L mol^{-1} at temperatures of 287, 298, 310 and 318 K, respectively. The FTIR spectra revealed that the protein secondary structure changed, with reductions in α-helices of about 3.65% at a drug to protein molar ratio of 3. The thermodynamic analysis (enthalpy and entropy change: ΔH^0 and ΔS^0) and the computational modelling study indicated that hydrophobic force played an important role in eupatilin–HSA complex stabilization, and eupatilin could bind within the subdomain IIA of HSA.

Introduction

Human serum albumin (HSA) has many important physiological functions and is one of the most extensively studied of all proteins (Shobini et al 2001; Haldar et al 2005). It is the most abundant carrier protein for many endogenous and exogenous substances in the blood (Kragh-Hansen 1981; Benet et al 1996). The main role of HSA in drug pharmacokinetics and pharmacodynamics relates to its ability to bind a large variety of drugs. Its primary pharmacokinetic function is participation in absorption, distribution, metabolism and excretion of drugs, because most drugs travel in the plasma and reach target tissues by binding to HSA (Neault & Tajmir-Riahi 1998; Caravan et al 2002; Pang et al 2005). Studies on the binding of drugs to HSA may provide useful information on the structural features that determine the therapeutic effectiveness of such drugs.

Flavonoids are a class of chemically related natural polyphenol products widely distributed in plants (Mabry et al 1970; Harborne 1976, 1988). Recently, much attention has been focused on their protective biochemical functions, important therapeutic applications (e.g. anticancer, antitumour, anti-inflammatory, anticoagulant, antioxidative effects) and their mechanisms of action (Havsteen 1983; Lamson & Brignall 2000; Middleton et al 2000). A number of biochemical and molecular biological investigations have revealed that proteins are frequently the targets for therapeutically active flavonoids of both natural and synthetic origin (Lamson & Brignall 2000; Sengupta & Sengupta 2002). In recent years, many studies have been carried out to investigate the interaction of HSA with flavonoids using fluorescence spectroscopy (Papadopoulou et al 2005; Sengupta et al 2005), Fourier transform infrared (FTIR) spectroscopy, circular dichroism spectroscopy (Tian et al 2004a, b) and molecular modelling (Zsila et al 2003). Eupatilin (5,7-dihydroxy-3′,4′,6-trimethoxyflavone; Figure 1) is one of the bioactive components isolated from *Artemisia* plants. As with other flavonoid compounds, this drug is increasingly being recognized as possessing pharmacological activity, including inhibitory effects on the viability and DNA synthesis capability of

School of Chemistry and Chemical Engineering, Jiangsu Teachers University of Technology, Key Laboratory of Precious Metal Chemistry and Technology of Jiangsu Province, Changzhou 213001, China

Jianghong Tang, Ning Lian, Chenglu Bi, Weihua Li

Correspondence: Jianghong Tang, School of Chemistry and Chemical Engineering, Jiangsu Teachers University of Technology, Yu Ying Road 2, Changzhou, Jiangsu, 213001, China. E-mail: tjh01@jstu.edu.cn

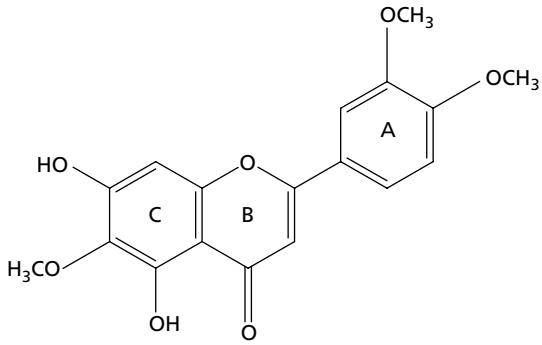

Figure 1 Chemical structure of eupatilin.

human promyelocytic leukaemia cells (Seo & Surh 2001), the cytostatic effects of human breast epithelial cells (Kim et al 2004), and selective inhibition of 5-lipoxygenase (Koshihara et al 1983). To date, the binding of eupatilin to HSA has not been studied. In the present work, we studied the interaction of eupatilin with HSA using fluorescence spectroscopy in combination with UV absorption spectroscopy and FTIR spectroscopy at simulative physiological pH. The location of eupatilin binding to HSA was determined by molecular modelling.

Materials and Methods

Materials

HSA (70024-90-7, 98% purity) was purchased from Sigma Chemical Company (St. Louis, MO, USA) and used without further purification; its molecular weight was assumed to be 66 500. Eupatilin (analytical grade) was purchased from The National Institute for the Control of Pharmaceutical and Biological Products (Beijing, China). Tris(hydroxymethylaminomethane) was of biochemical grade and was purchased from The Shanghai Chemical Reagent Head Factory (Shanghai, China). Analytical grade NaCl solution ($1.0\,mol\,L^{-1}$) was used to keep the ion strength at 0.1. Tris-HCl buffer solution ($0.05\,mol\,L^{-1}$) containing $0.1\,mol\,L^{-1}$ NaCl was used to keep the pH of the solution at 7.40. The HSA stock solution ($3.0\times10^{-5}\,mol\,L^{-1}$) was prepared in pH 7.40 Tris-HCl buffer solution and kept in the dark at 4 °C. The stock solution of eupatilin ($1.0\times10^{-3}\,mol\,L^{-1}$) was prepared in anhydrous methanol. All other reagents were of analytical grade and double distilled water was used in all experiments.

Apparatus and methods

The absorption spectra of eupatilin, HSA and the eupatilin–HSA complex were recorded on a CARY-100 UV-visible spectrophotometer (Varian, Inc., Palo Alto, CA, USA) at room temperature. A 1.0-cm quartz cell was used and the scanning wavelength ranged from 190 to 400 nm.

Fluorescence emission spectra were recorded in a RF-5301PC spectrofluorimeter (Shimadzu, Kyoto, Japan). Both excitation and emission bandwidths were set at 5 nm. The excitation wavelength was 280 nm, and the emission wavelengths were read over the range of 290–500 nm. For the fluorescence titration experiments 3.0 mL solution containing $3.0\times10^{-6}\,mol\,L^{-1}$ HSA was titrated in pH 7.4 Tris-HCl buffer solution by successive additions of stock solution of eupatilin (the eupatilin concentration range was from 6.0×10^{-6} to $1.90\times10^{-5}\,mol\,L^{-1}$). Each measurement was repeated in quintuplicate and the mean and standard deviation calculated. Eupatilin was added from concentrated stock solution so that the volume increment was negligible. Titrations were done manually by using trace syringes, and the fluorescence intensities were recorded at excitation and emission wavelengths of 280 and 336 nm, respectively. All experiments were performed at four temperatures (287, 298, 310 and 318 K). An electronic thermoregulating waterbath (NTT-2100; Eyela, Kyoto, Japan) was used for controlling the temperature.

FTIR measurements were performed at room temperature on a Nicolet Nexus 670 FTIR spectrometer (Nicolet, Madison, WI, USA) equipped with a germanium attenuated total reflection accessory, a deuterated triglycine sulfate detector and a KBr beam splitter. All spectra were obtained via the attenuated total reflection method with a resolution of $4\,cm^{-1}$ and 60 scans. The infrared spectra of HSA and the eupatilin–HSA complex (the molar ratio of eupatilin to HSA was 3:1) were obtained in the featured region of $1800–1300\,cm^{-1}$. The FTIR spectrum of free HSA was acquired by subtracting the absorption of the Tris buffer solution from the spectrum of the protein solution, and the difference spectrum of HSA was obtained by subtracting the spectrum of the eupatilin-free form from that of eupatilin–HSA form with the same concentrations. The subtraction criterion was that the original spectrum of the protein solution between 2200 and $1800\,cm^{-1}$ was featureless (Dong et al 1990). Fourier self-deconvolution and secondary derivative were applied over the range of $1600–1700\,cm^{-1}$ (amide I of HSA) to estimate the number, position and the width of component bands. Based on these parameters, a curve-fitting process was carried out using Galactic Peaksolve software (version 1.0; Galactic Industries Corp., Salem, NH, USA) to get the best Gaussian-shaped curves to fit the original protein spectra. After identification of the individual bands, the content of each representative structure of HSA was calculated using the area of their respective component bands.

The molecular modelling was carried out using the SYBYL 6.9 package on a SGI Fuel (Tripos, St. Louis, MO, USA) workstation. The crystal structure of HSA in a complex with R-warfarin was taken from the Brookhaven Protein Data Bank (entry codes 1 h9z) (Petitpas et al 2001). The potential of the 3-D structure of HSA was assigned according to the Amber 4.0 force field with Kollman-all-atom charges. The initial structures of eupatilin were generated by the molecular modelling software SYBYL 6.9. The geometry of the eupatilin molecule was subsequently optimized to minimal energy using the Tripos force field with Gasteiger-Marsili charges. Then, it was used to replace warfarin in the HAS–warfarin crystal structure. Finally, the FlexX program (included in SYBYL package) was used to establish the possible conformation of the ligands that bind to HSA.

Statistical analysis

Statistical analysis of the effect of temperature on the various binding parameters was performed using a one-way analysis of variance. Individual differences between the various temperatures were examined using Tukey's test. A value of

$P < 0.05$ denoted statistical significance in all cases. All results are expressed as mean ± s.d.

Results and Discussion

Binding properties of eupatilin to HSA

To analyse the binding properties (including the binding mechanism, binding constants, the number of binding sites, and the binding mode) of eupatilin to HSA, the fluorescence emission spectra of HSA in the absence and presence of eupatilin were collected (Figure 2). In the molecular structure of HSA, there are three intrinsic fluorophores: tryptophan, tyrosine and phenylalanine. At an excitation wavelength of 280 nm, tryptophan (and also tyrosine) residues are excited. The contribution of the fluorescence emission of tyrosine to the fluorescence emission of HSA at the maximal emission of tryptophan is very small. So the intrinsic fluorescence of HSA is almost exclusively contributed to by tryptophan at an excitation wavelength of 280 nm. From Figure 2, it can be seen that HSA had a strong fluorescence emission band, whereas eupatilin had no intrinsic fluorescence, at an excitation wavelength of 280 nm. With a gradual increase of eupatilin concentrations, the fluorescence intensity of HSA decreased regularly. This phenomenon suggested that the binding of eupatilin to HSA changed the microenvironment of the tryptophan residue of HSA (Yuan et al 1998).

Figure 3 shows the UV absorption spectra of eupatilin, HSA and the eupatilin–HSA complex. The absorption band at 210 nm of HSA is the characteristic of the α-helix structure of HSA. It can be seen from Figure 3 that the maximum absorption wavelengths of eupatilin, HSA and the eupatilin–HSA complex were different. Clearly, HSA had strong absorbance, with a peak at 209 nm, and the maximum absorbance wavelengths (211 nm) of the eupatilin–HSA complex increased with increasing concentrations of eupatilin. The absorbance of eupatilin solution (3.0×10^{-6} mol L^{-1}) and HSA solution (3.0×10^{-6} mol L^{-1}) at a wavelength of 209 nm was approximately

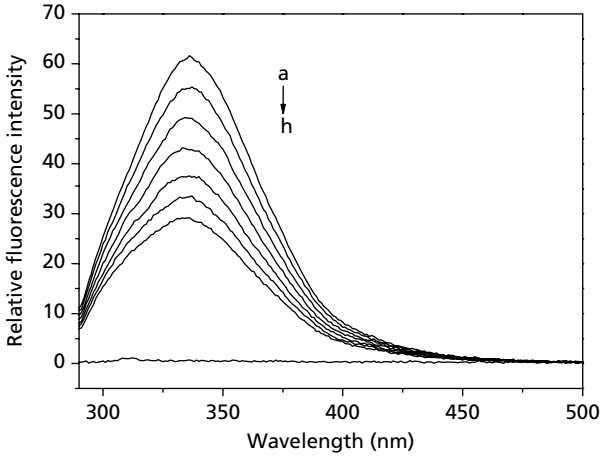

Figure 2 Fluorescence emission spectra of the HSA–eupatilin system. a. 3.0×10^{-6} mol L^{-1} HSA; b–g. 3.0×10^{-6} mol L^{-1} HSA in the presence of 0.50, 0.60, 0.70, 0.80, 0.90, 1.10×10^{-5} mol L^{-1} eupatilin, respectively; h. 1.0×10^{-5} mol L^{-1} eupatilin. pH 7.4, $\lambda_{ex} = 280$ nm, T = 287 K.

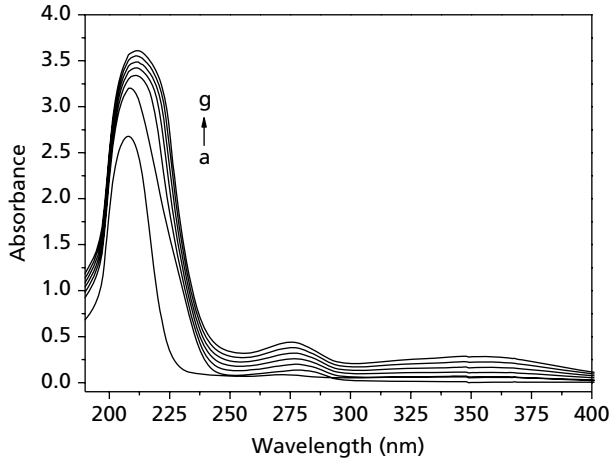

Figure 3 UV absorbance spectra obtained in Tris buffer solution (pH 7.4). a. eupatilin, 3.0×10^{-6} mol L^{-1}; b. HSA, 3.0×10^{-6} mol L^{-1}; c–g. eupatilin–HSA, 3.0×10^{-6} mol L^{-1} HSA in the presence of 3.0, 6.0, 9.0, 12, 15×10^{-6} mol L^{-1} eupatilin.

2.67 and 3.23, respectively. The absorbance of the eupatilin–HSA complex at 209 nm was 3.32. This result indicated that an interaction occurs between eupatilin and HSA, that is the formation of eupatilin–HSA complexes.

Data from the fluorescence titration experiments can be analysed according to the modified Stern-Volmer equation (Lackowicz 1999):

$$(F_0/(F_0 - F)) = (1/fK[Q]) + (1/f) \quad (1)$$

where F_0 and F are the relative fluorescence intensities of protein in the absence and presence of quencher, respectively, K is the Stern-Volmer quenching constant, [Q] is the quencher concentration, and f is the fractional maximum fluorescence intensity of protein summed up. The plot of $F_0/(F_0 - F)$ versus 1/[Q] is linear with 1/fK as the slope and 1/f as the intercept. The quenching constant K is a quotient of the intercept 1/f and slope 1/fK. The constant K calculated from the Stern-Volmer equation is given in Table 1. Statistical comparison indicated that increasing temperature had a significant effect on the quenching constant ($P < 0.05$). The quenching constant decreased with increasing temperature,

Table 1 Binding parameters for the eupatilin–human serum albumin complex at pH 7.4 measured by fluoremetric titrations

Temperature (K)	Stern-Volmer method	Scatchard method	
	K ($\times 10^5$ L mol^{-1})	K ($\times 10^5$ L mol^{-1})	n
287	1.51 ± 0.076*	1.53 ± 0.069*	1.17 ± 0.020
298	1.19 ± 0.043	1.20 ± 0.039	1.24 ± 0.012
310	1.01 ± 0.058	1.05 ± 0.049	1.28 ± 0.017
318	0.84 ± 0.053	0.87 ± 0.048	1.33 ± 0.019

Values are mean ± s.d. of five determinations. *$P < 0.05$, significantly different among four temperatures.

indicating a static type of quenching mechanism in which the quenching constant can be interpreted as the association constant of the complexation reaction because static quenching arises from the formation of a ground state complex that is non-fluorescent or weakly fluorescent between fluorophore and quencher (Eftink & Ghiron 1976).

In the drug–protein binding studies, the binding constants were also calculated using the Scatchard equation (Scatchard 1949):

$$r/D_f = nK - rK \quad (2)$$

where r represents the number of moles of bound drug per mole of protein, n is the number of binding sites, D_f represents the concentration of unbound drug, and K is the binding constant. The plot of r/D_f versus r gives the binding constant. The results are summarized in Table 1. Statistical comparison indicated that increasing temperature did not have a significant effect on the number of binding sites ($P<0.05$). The linearity of the Scatchard plot (not shown) indicated that eupatilin bound to a single class of binding site on HSA and the binding constants were consistent with those obtained by the modified Stern-Volmer equation. In this study, the binding constants obtained with the modified Stern-Volmer equation were applied in the discussion of binding modes.

Alterations of protein secondary structure induced by eupatilin

In order to obtain more binding information of eupatilin to HSA, the FTIR spectra were investigated, since infrared spectra of proteins exhibit a number of the amide bands, which represent different vibrations of peptide moieties. Among the amide bands of the protein, the amide I band ranging from 1600 to 1700 cm^{-1} (mainly C=O stretch) and the amide II band 1548 cm^{-1} (C-N stretch coupled with N-H bending mode) have been widely used (Sirotkin et al 2001). They both have a relationship with the secondary structure of the protein. However, the amide I band is more sensitive to the change of protein secondary structure than the amide II band (Rahmelow & Hubner 1996). The FTIR spectra and difference spectra of HSA are shown in Figure 4. From Figure 4 it can be seen that the peak positions of amide I bands shifted from 1656.40 to 1636.51 cm^{-1} in the HSA infrared spectrum after interaction with eupatilin. The changes of these peak positions and peak shapes demonstrated the secondary structures of HSA were changed by the interaction of eupatilin with HSA.

For the quantitative analysis of each secondary structure, the origin spectra of amide I bands of free HSA and the HSA–eupatilin complex in Tris-HCl buffer were treated with Fourier self-deconvolution and second derivative to estimate the number and position of component bands (figure not shown). According to Jiang et al (2004), before estimation of the percentage content of each secondary structure, the component bands should be assigned. Bands over the range 1610–1640 cm^{-1} are generally assigned to β-sheet, 1640–1650 cm^{-1} to random coil, 1650–1658 cm^{-1} to α-helix and 1660–1700 cm^{-1} to β-turn structure. The percentages of each secondary structure of HSA can be calculated based on the integrated areas of the component bands in amide I. The free HSA contained

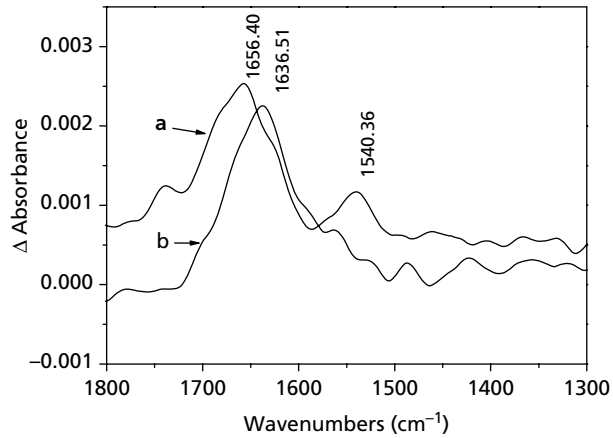

Figure 4 FTIR spectra and difference spectra of HSA. a. The FTIR spectra of free HSA (subtracting the absorption of the buffer solution from the spectrum of the protein solution); b. the FTIR difference spectra of HSA (subtracting the absorption of the eupatilin-free form from that of eupatilin–HSA bound form). Tris-HCl buffer, pH 7.4, ionic strength 0.1, $C_{HSA} = 3.0 \times 10^{-6}$ mol L^{-1}, $C_{eupatilin} = 9.0 \times 10^{-6}$ mol L^{-1}.

α-helical (50.93%), β-sheet (25.46%) and β-turn structures (23.61%). With regard to the eupatilin–HSA complex, the α-helical structure reduced from 50.93% to 47.25%, β-sheet from 25.46% to 15.93%, and β-turn increased from 23.61% to 36.81% after interaction of eupatilin with HSA.

Binding mode of eupatilin with HSA

When a small molecule is bound to a biomacromolecule there are several types of non-covalent interaction modes, such as hydrogen bond, van der Waals force, hydrophobic interaction force and electrostatic force (Timaseff 1972). The thermodynamic parameters of the binding reaction are the main evidence for the binding mode. For this purpose, the temperature-dependence of the binding constant was studied. The chosen temperatures were 287, 298, 310 and 318 K, at which HSA did not undergo any structural degradation. The thermodynamic parameters were analysed according to the following van't Hoff equation:

$$\ln K = -\Delta H^0/RT + \Delta S^0/R \quad (3)$$

$$\Delta G^0 = -RT \ln K \quad (4)$$

$$\Delta S^0 = (\Delta H^0 - \Delta G^0)/T \quad (5)$$

where K is the binding constant at the corresponding temperature, R is the gas constant, T is absolute temperature, and ΔH^0, ΔG^0 and ΔS^0 are enthalpy change, free energy change and entropy change, respectively. If the temperature changes a little, the enthalpy change ΔH^0 is regarded as a constant. The value of ΔH^0 can be obtained from the linear relationship between lnK and the reciprocal absolute temperature (1/T) (figure not shown). The ΔG^0 and ΔS^0 at different temperatures were calculated using Equations 4 and 5 and the results are given in Table 2. As shown in Table 2, the negative sign for ΔG^0 meant that the binding process was spontaneous and

Table 2 Thermodynamic parameters for the binding of eupatilin to human serum albumin at pH 7.4

Temperature (K)	ΔG^0 (kJ mol^{-1})	ΔH^0 (kJ mol^{-1})	ΔS^0 (J mol^{-1} K^{-1})
287	−28.44 ± 0.069	−13.76 ± 0.048	51.15 ± 0.030
298	−28.97 ± 0.041	−13.76 ± 0.048	51.04 ± 0.028
310	−29.69 ± 0.050	−13.76 ± 0.048	51.28 ± 0.022
318	−29.97 ± 0.051	−13.76 ± 0.048	51.00 ± 0.031

Values are mean ± s.d. of five determinations. ΔH^0, ΔG^0 and ΔS^0 are enthalpy change, free energy change and entropy change.

the formation of the eupatilin–HSA complex was an exothermic reaction accompanied with negative enthalpy change (−13.76 kJ mol^{-1}) and positive entropy change (51.04 J mol^{-1} K^{-1}, 298 K). The sign and magnitude of the thermodynamic parameters associated with various individual kinds of interactions that may take place in protein association processes were characterized (Ross & Subramanian 1981; Mohammed et al 1993). From the point of view of water structure, positive entropy change is generally considered as the evidence for hydrophobic interactions. In addition, a specific electrostatic interaction among ionic species in an aqueous solution is characterized by a positive ΔS^0 value and negative ΔH^0 value. Thus, it was impossible to demonstrate the thermodynamic parameters of the eupatilin–HSA complex compound on the basis of a single intermolecular force model. It was more likely that hydrophobic and electrostatic interactions were involved in its binding process. However, under the conditions here (pH 7.40) eupatilin might be considered largely un-ionized according to its structure. Thus, electrostatic interaction cannot play a main role in the binding process. In the binding process of eupatilin to HSA, the ΔG^0 value mainly depended on the contribution of ΔS^0, with little contribution of the ΔH^0 value, so the hydrophobic interaction might play a main role in the interaction of eupatilin with HSA, but the electrostatic interaction cannot be excluded.

Computational modelling study of the interaction between eupatilin and HSA

It is well known that HSA is a monomeric protein comprising 585 amino acids. The investigations of 3-D structure of crystalline albumin showed that HSA contains three homologous domains (I, II, III): I (residues 1–195), II (residues 196–383), III (residues 384–585), and each domain can be divided into two subdomains (A and B) (Sjoholm et al 1979). The crystallographic analysis (He & Carter 1992; Curry et al 1998) revealed that HSA has drug binding sites within hydrophobic cavities in subdomains IIA and IIIA, which correspond to site I and site II, respectively, and the sole tryptophan residue (Trp-214) of HSA is in subdomain IIA. There is a large hydrophobic cavity present in subdomain IIA that many drugs can bind.

In order to further study the binding mode and binding location of eupatilin to HSA, the SGI Fuel workstation was used for the computational modelling study. The optimal energy ranked result is shown in Figure 5. It can be seen that the eupatilin molecule was situated within the subdomain IIA hydrophobic cavity. The drug molecule moiety was located

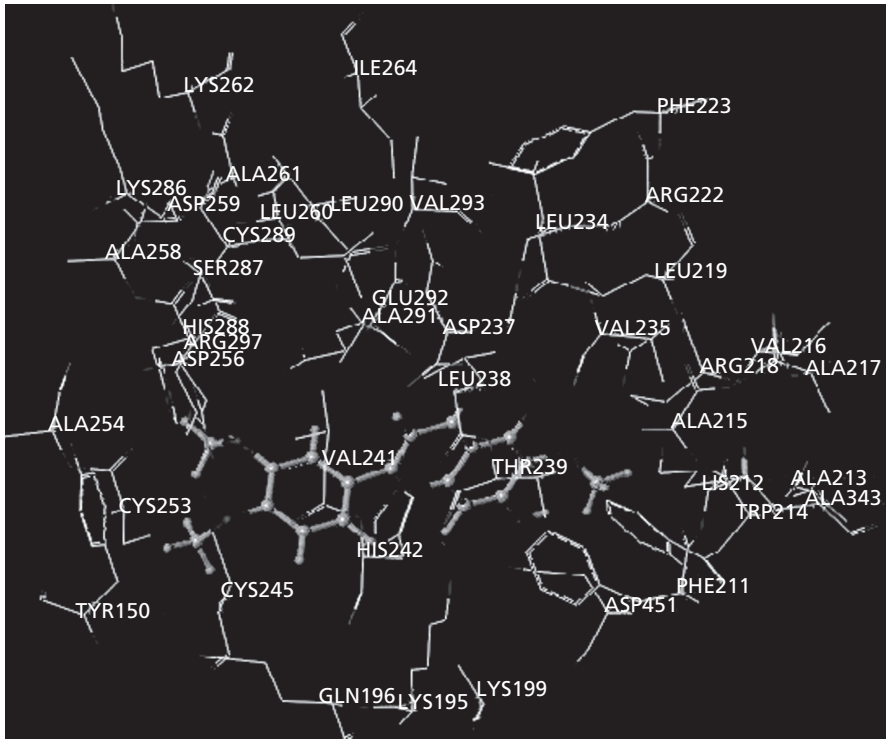

Figure 5 Interaction mode between eupatilin and HAS; only residues around 8 Å of the ligand are displayed. The residues of HSA are represented by lines and the ligand structure is represented by the ball-and-stick model.

within the binding pocket and the B- and C-rings were coplanar. The B- and C-rings of the eupatilin molecule were inserted in the hydrophobic cavity of site I, and it is important to note that the tryptophan residue of HSA (Try-214) was in close proximity to the methoxy of the C-ring of eupatilin, suggesting the existence of a hydrophobic interaction between them. Furthermore, this finding provided a good structural basis to explain the very efficient fluorescence quenching of HSA emissions in the presence of eupatilin. The results of molecular modelling suggested that the interaction between HSA and eupatilin was dominated by hydrophobic force, which was in agreement with the binding mode proposed in this article.

Conclusion

Some researches have suggested that HSA can bind many ligands at several binding sites. Site I of HSA showed an affinity for warfarin (Sudlow et al 1976), bilirubin (Chen 1974) and salicylate (Ozer & Taca 2001); these molecules quenched HSA fluorescence through a static mechanism and the hydrophobic interaction was the main force between HSA and the quencher. In this study, the mechanism of the eupatilin interaction with HSA was investigated by fluorescence spectroscopy and UV absorbance combined with FTIR spectrophotometric techniques under simulative physiological conditions. The experimental results suggested that the intrinsic fluorescence of HSA was quenched through static mode and the binding of eupatilin to HSA was mainly based on the hydrophobic force. The eupatilin molecule was bound to HSA via a single class of binding site. The FTIR spectra revealed that the protein secondary structure changed after the eupatilin interaction with HSA. Computational modelling of the eupatilin–HSA complex suggested that eupatilin bound within the subdomain IIA of the protein.

References

Benet, L. Z., Kroetz, D. L., Sheiner, L. B. (1996) The dynamics of drug absorption distribution and elimination. In: Goodman, G. A., Gilman, R. H. (eds) *The Pharmacological basis of therapeutics*, 9th edn. McGraw-Hill, New York, pp 3–27

Caravan, P., Cloutier, N. J., Greenfield, M. T. (2002) The interaction of MS-325 with human serum albumin and its effect on proton relaxation rates. *J. Am. Chem. Soc*. **124**: 3152–3162

Chen, R. F. (1974) Fluorescence stopped-flow study of relaxation processes in the binding of bilirubin to serum albumins. *Arch. Biochem. Biophys*. **160**: 106–112

Curry, S., Mandelkow, H., Brick, P., Franks, N. (1998) Crystal structure of human serum albumin complexed with fatty acid reveals an asymmetric distribution of binding sites. *Nat. Struct. Biol*. **5**: 827–835

Dong, A., Huang, P., Caughey, W. S. (1990) Protein secondary structures in water from second derivative amide I infrared spectra. *Biochemistry* **29**: 3303–3308

Eftink, M. R., Ghiron, C. A. (1976) Fluorescence quenching of indole and model micelle systems. *J. Phys. Chem*. **80**: 486–493

Haldar, B., Mallick, A., Chattopadhyay, N. (2005) Interaction of pyrene-end-capped poly (ethylene oxide) with bovine serum albumin and human serum albumin in aqueous buffer medium: a fluorometric study. *J. Photochem. Photobiol. B* **80**: 217–224

Harborne, J. B. (1976) Functions of flavonoids in plants. In: Goodwin, T. W. (ed.) *Chemistry and biochemistry of plant pigments*. Academic Press, London, pp 736–779

Harborne, J. B. (1988) Flavonoids in the environment: structure–activity relationships. In: Cody, V., Middleton, E., Harborne, J. B., Beretz, A. (eds). *Plant flavonoids in biology and medicine. II. Biochemical, cellular and medicinal properties*. Alan R Liss, New York, pp 17–27

Havsteen, B. (1983) Flavonoids: a class of natural products of high pharmacological potency. *Biochem. Pharmacol*. **32**: 1141–1148

He, J. X., Carter, D. C. (1992) Atomic structure and chemistry of human serum albumin. *Nature* **358**: 209–215

Jiang, M., Xie, M. X., Zheng, D., Liu, Y., Li, X. Y., Chen, X. (2004) Spectroscopic studies on the interaction of cinnamic acid and its hydroxyl derivatives with human serum albumin. *J. Mol. Struct*. **692**: 71–80

Kim, D. H., Na, H. K., Oh, T. Y., Kim, W. B., Surh, Y. J. (2004) Eupatilin, a pharmacologically active flavone derived from Artemisia plants, induces cell cycle arrest in ras-transformed human mammary epithelial cells. *Biochem. Pharmacol*. **68**: 1081–1087

Koshihara, Y., Neichi, T., Murota, S. I., Lao, A. N., Fujimoto, Y., Tatsuno, T. (1983) Selective inhibition of 5-lipoxygenase by natural compounds isolated from Chinese plants, Artemisia rubripes Nakai. *FEBS lett*. **158**: 41–44

Kragh-Hansen, U. (1981) Molecular aspects of ligand binding to serum albumin. *Pharmacol. Rev*. **33**: 17–53

Lackowicz, J. R. (1999) *Principles of fluorescence spectroscopy*, 2nd edn. Kluwer/Plenum, New York

Lamson, S. W., Brignall, M. S. (2000) Antioxidants and cancer, part 3: quercetin. *Altern. Med. Rev*. **5**: 196–208

Mabry, T. J., Markham, K. R., Thomas, M. B. (1970) *The systematic identification of flavonoids*. Springer-Verlag, Heidelberg, New York, Berlin

Middleton, J. E., Kandaswami, C., Theoharides, T. C. (2000) The effects of plant flavonoids on mammalian cells: implications for inflammation, heart disease, and cancer. *Pharmacol. Rev*. **52**: 673–751

Mohammed, H. R., Toru, M., Tomoko, O., Keishi, Y., Masaki, O. (1993) Study of interaction of carprofen and its enantiomers with human serum albumin: mechanism of binding studied by dialysis and spectroscopic methods. *Biochem. Pharmacol*. **46**: 1721–1731

Neault, J. F., Tajmir-Riahi, H. A. (1998) Interaction of cisplatin with human serum albumin. Drug binding mode and protein secondary structure. *Biochim. Biophys. Acta* **1384**: 153–159

Ozer, I., Taca, O. (2001) Method dependence of apparent stoichiometry in the binding of salicylate ion to human serum albumin: a comparison between equilibrium dialysis and fluorescence titration. *Anal. Biochem*. **294**: 1–6

Pang, Y. H., Yang, L. L., Shuang, S. M., Dong, C., Thompson, M. (2005) Interaction of human serum albumin with bendroflumethiazide studied by fluorescence spectroscopy. *J. Photochem. Photobiol. B* **80**: 139–144

Papadopoulou, A., Green, R. J., Frazier, R. A. (2005) Interaction of flavonoids with bovine serum albumin: a fluorescence quenching study. *J. Agric. Food Chem*. **53**: 158–163

Petitpas, I., Bhattacharya, A. A., Twine, S., East, M., Curry, S. (2001) Crystal structure analysis of warfarin binding to human serum albumin. *J. Biol. Chem*. **276**: 22 804–22 809

Rahmelow, K., Hubner, W. (1996) Secondary structure determination of proteins in aqueous solution by infrared spectroscopy. A comparison of multivariate data analysis. *Anal. Biochem*. **241**: 5–11

Ross, D. P., Subramanian, S. (1981) Thermodynamics of protein association reactions: forced contributing to stability. *Biochemistry* **20**: 3096–3102

Scatchard, G. (1949) The attractions of protein for small molecules and ions. *Ann. N. Y Acad. Sci*. **51**: 660–672

Seo, H. J., Surh, Y. J. (2001) Eupatilin, a pharmacologically active flavone derived from *Artemisia* plants, induces apoptosis in human promyelocytic leukemia cells. *Mutat. Res.-Gen. Tox. En*. **496**: 191–198

Sengupta, B., Sengupta, P. K. (2002) The interaction of quercetin with human serum albumin: a fluorescence spectroscopic study. *Biochem. Biophys. Res. Commun*. **299**: 400–403

Sengupta, B., Banerjee, A., Sengupta, P. K. (2005) Interactions of the plant flavonoid fisetin with macromolecular targets: insights from fluorescence spectroscopic studies. *J. Photochem. Photobiol. B* **80**: 79–86

Shobini, J., Mishra, A. K., Sandhya, K., Chandra, N. (2001) Interaction of coumarin derivatives with human serum albumin: investigation by fluorescence spectroscopic technique and modeling studies. *Spectrochim. Acta A* **57**: 1133–1147

Sirotkin, V. A., Zinatullin, A. N., Solomonov, B. N., Faizullin, D. A., Fedotov, V. D. (2001) Calorimetric and Fourier transform infrared spectroscopic study of solid proteins immersed in low water organic solvents. *Biochim. Biophys. Acta* **1547**: 359–369

Sjoholm, I., Ekman, B., Kober, A., Ljungstedt-Pahlman, I., Seiving, B., Sjodin, T. (1979) Binding of drugs to human serum albumin: XI. The specificity of three binding sites as studied with albumin immobilized in microparticles. *Mol. Pharmacol*. **16**: 767–777

Sudlow, G., Birkett, D. J., Wade, D. N. (1976) Further characterization of specific drug binding site on human serum albumin. *Mol. Pharmacol*. **12**: 1052–1061

Tian, J. N., Liu, J. Q., He, W. Y., Hu, Z. D., Yao, X. J., Chen, X. G. (2004a) Probing the binding of scutellarin to human serum albumin by circular dichroism, fluorescence spectroscopy, FTIR, and molecular modeling method. *Biomacromolecules* **5**: 1956–1961

Tian, J. N., Liu, J. Q., Xie, J. P., Yao, X. J., Hu, Z. D., Chen, X. G. (2004b) Binding of wogonin to human serum albumin: a common binding site of wogonin in subdomain IIA. *J. Photochem. Photobiol. B* **74**: 39–45

Timaseff, S. N. (1972) Thermodynamics of protein interactions. In: Peeters, H. (ed.) *Proteins of biological fluids*. Pergamon Press, Oxford, pp 511–522

Yuan, T., Weljie, A. M., Vogel, H. J. (1998) Tryptophan fluorescence quenching by methionine and selenomethionine residues of calmodulin: orientation of peptide and protein binding. *Biochemistry* **37**: 3187–3195

Zsila, F., Bikádi, Z., Simonyi, M. (2003) Probing the binding of the flavonoid quercetin to human serum albumin by circular dichroism, electronic absorption spectroscopy and molecular modeling methods. *Biochem. Pharmacol*. **65**: 447–456